Journal of Molecular Structure 1324 (2025) 140803

Contents lists available at ScienceDirect

Journal of Molecular Structure

journal homepage: www.elsevier.com/locate/molstr

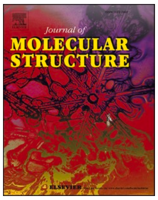

Synthesis of a wide range of biphenyl derivatives and symmetrical sulfides, using $SnFe_2O_4$@SiO_2@P-Pd MNPs as a novel, efficient, green, and reusable catalyst

Anjan Kumar [a,*], Jayanti Makasana [b], Suhas Ballal [c], Hamidah Abu Bakar [d], Girish Chandra Sharma [e], RSK Sharma [f], Lakshay Bareja [g], Salwa Bader AlReshaidan [h], Mohammed A. El-Meligy [i,j], Munthar Kadhim Abosaoda [k,l]

[a] *Department of Electronics and Communication Engineering, GLA University, Mathura- 281406, India*
[b] *Marwadi University Research Center, Department of Chemistry, Faculty of Science Marwadi University, Rajkot, 360003, Gujarat, India*
[c] *Department of Chemistry and Biochemistry, School of Sciences, JAIN (Deemed to be University), Bangalore, Karnataka, India*
[d] *Management and Science University, Shah Alam, Selangor, Malaysia*
[e] *Department of Applied Sciences-Chemistry, NIMS Institute of Engineering & Technology, NIMS University Rajasthan, Jaipur, India*
[f] *Department of Chemistry, Raghu Engineering College, Visakhapatnam, Andhra Pradesh 531162, India*
[g] *Centre for Research Impact & Outcome, Chitkara University Institute of Engineering and Technology, Chitkara University, Rajpura 140401, Punjab, India*
[h] *Department of Chemistry, Faculty of Science, King Saud University, P.O. Box 800, Riyadh 11451, Saudi Arabia*
[i] *Jadara University Research Center, Jadara University, Jordan*
[j] *Applied Science Research Center, Applied Science Private University, Amman, Jordan*
[k] *College of pharmacy, the Islamic University, Najaf, Iraq*
[l] *College of pharmacy, the Islamic University of Al Diwaniyah, Al Diwaniyah, Iraq*

ARTICLE INFO

Keywords:
Sulfides
Cross-coupling
Biphenyl
$SnFe_2O_4$

ABSTRACT

We have introduced the $SnFe_2O_4$@SiO_2@P-Pd catalyst for the one-pot synthesis of biphenyl derivatives and symmetrical sulfides. For this purpose, $SnFe_2O_4$ nanoparticles were modified with Phenylalanine. The synthesized catalyst underwent characterization through BET, FT-IR, SEM, XRD, ICP, TGA, VSM, and EDX analyses. This novel approach offers the advantages of a recyclable heterogeneous catalyst, which can be easily separated from the reaction mixture using an external magnet, along with shorter reaction times, high product yields, and cost-effective, environmentally friendly conditions. The $SnFe_2O_4$@SiO_2@P-Pd catalyst can be reused for up to five cycles without significant loss of catalytic activity. The results indicate that $SnFe_2O_4$@SiO_2@P-Pd is an effective hybrid catalyst for synthesizing biphenyl derivatives and symmetrical sulfides.

1. Introduction

One of the primary goals in transition metal-catalyzed organic synthesis is the formation of carbon–carbon (C–C) bonds [1]. The Pd-catalyzed Stille coupling (St) coupling reaction is regarded as one of the most effective techniques for constructing these bonds [2]. While numerous approaches such as Kharash coupling, Stille coupling, Negishi coupling, Himaya coupling, and Kumuda coupling exist for synthesizing biaryls, the St cross-coupling reaction has recently emerged as the most favored method. This preference for the St cross-coupling reaction over other palladium-catalyzed alternatives is not coincidental [3]. The primary advantages of the St coupling lie in its mild reaction conditions and the straightforward accessibility to a variety of commercially available boronic acids. These acids are more environmentally friendly than other organometallic reagents [4]. Palladium is particularly versatile among nanocatalysts used in forming carbon-carbon bonds through coupling reactions like Stille and Sonogashira. This versatility makes it the most commonly used nanocatalyst in these processes [5]. The creation of carbon-sulfur and carbon-carbon bonds is a crucial and effective method for synthesizing diverse compounds used in agriculture, pharmaceuticals, and electronic materials [6,7]. Researchers are highly interested in sulfur-containing compounds due to their natural abundance and their role as essential elements in biologically and medicinally active substances [8]. These compounds serve various purposes, ranging from

---

* Corresponding author.
E-mail address: dranjan.nitp@gmail.com (A. Kumar).

https://doi.org/10.1016/j.molstruc.2024.140803
Received 6 October 2024; Received in revised form 17 November 2024; Accepted 18 November 2024

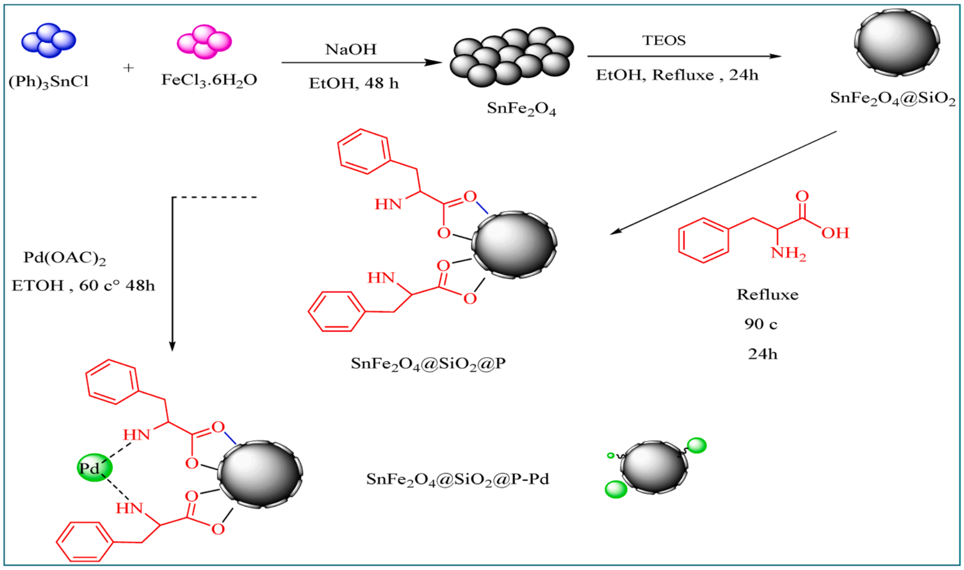

Scheme 1. Synthesis of $SnFe_2O_4@SiO_2@P\text{-}Pd$.

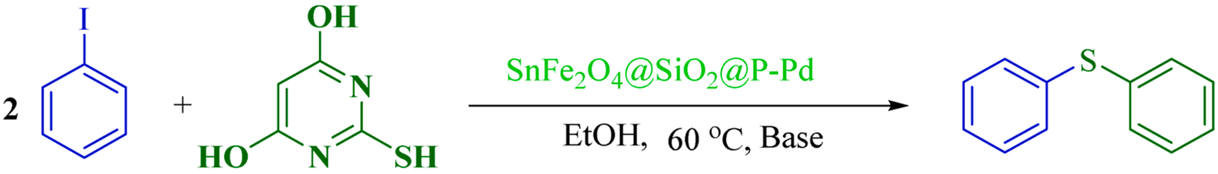

Scheme 2. Synthesis of symmetrical sulfides catalyzed by $SnFe_2O_4@SiO_2@P\text{-}Pd$.

starting materials to valuable intermediates in organic reactions [9]. Symmetrical and unsymmetrical sulfides, along with their sulfoxide counterparts, have found extensive use as solvents, glycosyl donors in oligosaccharide synthesis, and intermediates in total organic synthesis, as well as possessing antibacterial, antifungal, anti-atherosclerotic, and antihypertensive properties [10]. Consequently, developing new, efficient, and safe methods for producing sulfur-containing compounds is particularly important. Generally, the synthesis of symmetrical and unsymmetrical sulfoxides has been attempted through various methods [11]. These include reactions involving sulfur dioxide with organolithium or Grignard reagents, palladium-catalyzed arylation of alkyl and aryl sulfonate anions, reactions of aryl benzyl sulfoxides with aryl bromides, benzyl halides with DMSO, thiol additions to olefins and alkynes, the Reinheckel protocol, Heck vinylations, among others. However, many of these methods are restricted to a limited range of substrates and often require complex and harsh reaction conditions.

The formation of the carbon–sulfur bond is a critical chemical reaction with significant applications in medicinal chemistry, organic synthesis, and materials science. Transition metal-catalyzed cross-coupling of aryl halides with thiols is the most prevalent method for synthesizing diaryl sulfides. However, these C-S coupling reactions face major challenges due to the use of highly volatile, foul-smelling, and toxic thiols, posing health risks [12]. While several heterogeneous catalysts are reported for C-S coupling reactions, their recovery process is often complicated [13]. Consequently, magnetic catalysts have been suggested as an effective solution. To address these issues, recent advancements have introduced various sulfur sources for converting aryl halides to aryl thioesters using transition metal catalysts such as nickel or palladium nanoparticles [14]. In recent years, researchers have created a wide range of magnetic nanoparticles that are easy to recycle and separate. These developments make them highly effective catalysts in the synthesis of various organic compounds [15–18]. These magnetic nanoparticles can be effortlessly extracted from reaction mixtures using a basic bar magnet [19]. Notably, within the realm of heterogeneous catalysts, $SnFe_2O_4$ nanoparticles have garnered significant attention due to their ease of synthesis and straightforward surface modification [20, 21].

In this study, as part of our research program aimed at developing environmentally friendly catalysts, we prepared $SnFe_2O_4@SiO_2@P\text{-}Pd$. We introduce this new green catalyst as an effective solution for the reaction of symmetric sulfides and biphenyl derivatives.

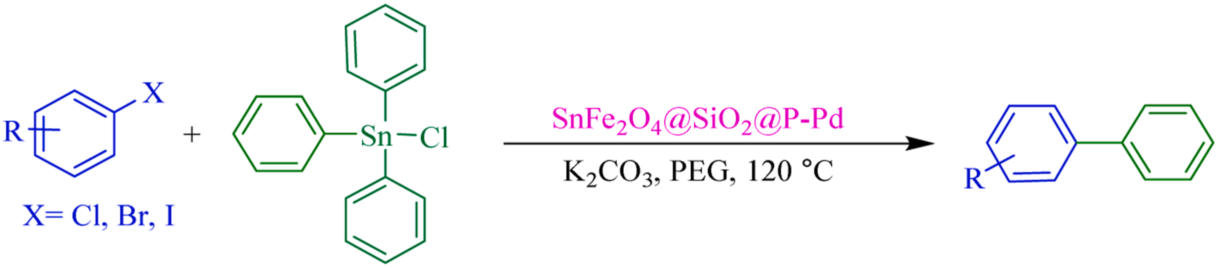

Scheme 3. Synthesis of Stille reaction catalyzed by $SnFe_2O_4@SiO_2@P\text{-}Pd$.

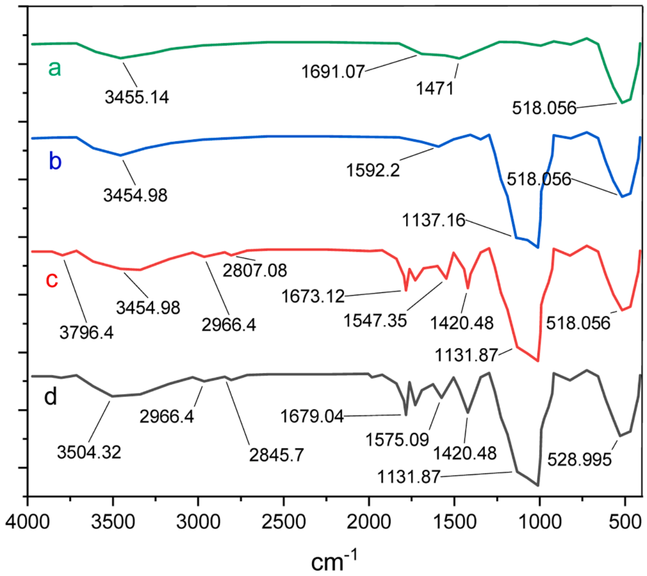

Fig. 1. Comparative study of FT-IR spectra of a) $SnFe_2O_4$, b) $SnFe_2O_4@SiO_2$, c) $SnFe_2O_4@SiO_2@P$, d) $SnFe_2O_4@SiO_2@P$-Pd.

2. Experimental

2.1. Chemicals and apparatus

The initial materials and solvents for this project were obtained from Fluka, Merck, or Sigma-Aldrich and were used as is, without further purification. Thin-layer chromatography was carried out using Merck GF254 silica gel plates. The FT-IR spectra were recorded with a Bruker FT-IR model Tensor 27 spectrometer using KBr discs within the 400–4000 cm^{-1} range. XRD patterns were obtained using a PANalytical X'Pert PRO instrument for X-ray diffraction (XRD) analysis. A thermogravimetric analysis (TGA) was performed using a T.A. model Q600 instrument. Magnetic properties were assessed using vibrating sample magnetometry (VSM) with a Lake Shore 7200 at 300 KVsm. The LBKFB PerkinElmer model was employed for inductively coupled plasma (ICP) analysis. Melting points were determined using a Bu¨chi B-545 apparatus with open capillary tubes. Images from the scanning electron microscope were captured using the LEO 1430 VP. The 1 H NMR spectra (400 MHz, DMSO-d_6) were obtained using BRUKER AVANCE equipment with DMSO-d_6 as the solvent.

2.2. Preparation of $SnFe_2O_4@SiO_2@P$-Pd

The synthesis of $SnFe_2O_4@SiO_2@P$-Pd magnetic nanoparticles (MNPs) commenced with the preparation of $SnFe_2O_4@SiO_2$, following methodologies detailed in earlier studies (refer to Scheme 1). To synthesize the $SnFe_2O_4@SiO_2@P$ complex, 3 gs of the previously prepared $SnFe_2O_4@SiO_2$ were dispersed in 60 mL of toluene via sonication for a duration of 35 min. Subsequently, 3 millimoles of Phenylalanine (P) were introduced into the flask, which was then stirred at 90 °Celsius for 60 h. Upon completion of the reaction, the resulting $SnFe_2O_4@SiO_2@P$ complex was separated through magnetic isolation, followed by washing with ethyl acetate and water. The product was then dried at 65 °Celsius for 14 h. To synthesize the $SnFe_2O_4@SiO_2@P$-Pd complex, a combination of $SnFe_2O_4@SiO_2@P$ (1.5 gs), palladium (II) acetate (3 millimoles), and 50 mL of ethanol was placed in a flask and stirred at 60 °Celsius for 48 h under reflux conditions. Sodium borohydride (1.5 millimoles) was subsequently added to the mixture and stirred for an additional 5 h. Following the conclusion of the reaction, the $SnFe_2O_4@SiO_2@P$-Pd complex was isolated, washed with ethanol and water, and finally dried under vacuum at 65 °Celsius.

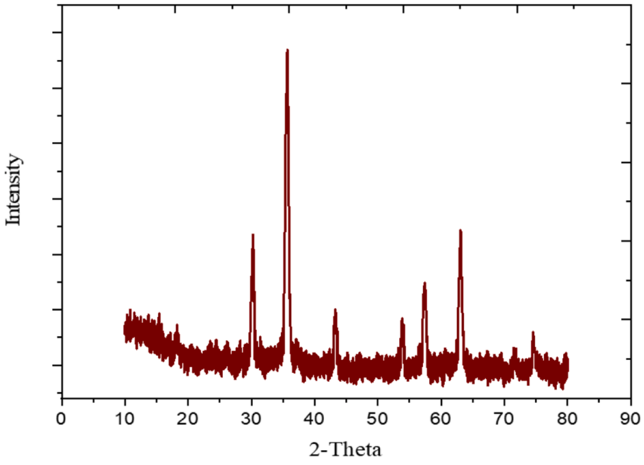

Fig. 2. XRD spectrum of $SnFe_2O_4@SiO_2@P$-Pd.

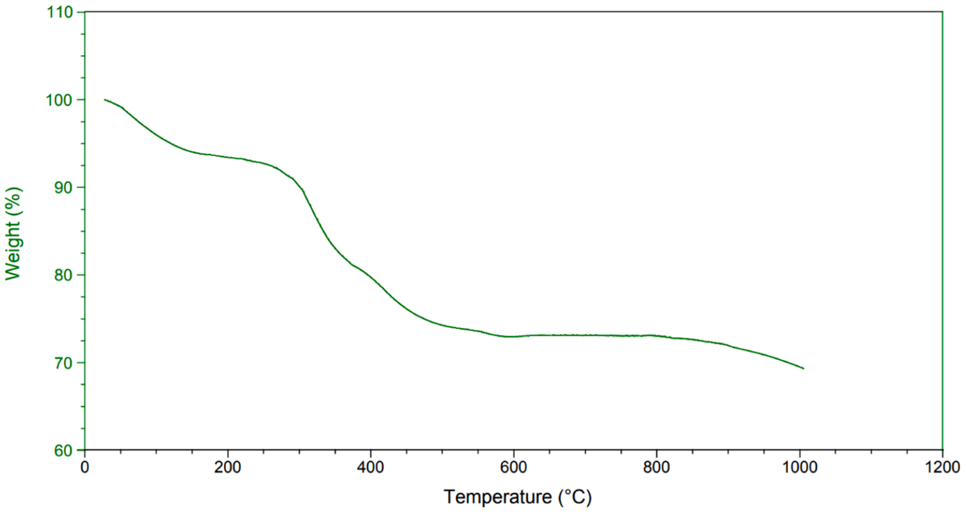

Fig. 3. TGA curve of $SnFe_2O_4@SiO_2@P\text{-}Pd$.

2.3. *Preparation of symmetrical sulfides*

In this study, 2-thiobarbituric acid (0.5 mmol), along with potassium hydroxide (KOH, 1 mmol) and an aryl halide (1 mmol), was dissolved in ethanol (3 mL). To this solution, $SnFe_2O_4@SiO_2@P\text{-}Pd$ (0.015 g) was added, and the resulting mixture was stirred under reflux conditions. Upon completion of the reaction, as confirmed by thin-layer chromatography (TLC), the catalyst was removed using a magnet and subsequently washed with ethyl acetate (3 × 8 mL). The desired product was then purified using silica gel column chromatography, as illustrated in Scheme 2.

2.4. *Preparation of stille reaction*

In an experimental setup, a mixture comprising triphenyltin chloride (0.6 mmol), aryl halides (0.5 mmol), and potassium carbonate (K_2CO_3, 0.7 mmol) was introduced into a flask alongside $SnFe_2O_4@SiO_2@P\text{-}Pd$ (0.015 g) as a catalyst. This reaction medium was dissolved in polyethylene glycol and subjected to stirring at 120 °C. The progress of the reaction was monitored through thin-layer chromatography (TLC) until completion was affirmed. Subsequently, the mixture was allowed to cool to ambient temperature, facilitating the separation of the catalyst using an external magnetic force. The solution obtained thereafter was extracted utilizing water and n-hexane, followed by drying over sodium sulfate (1.5 g). Post solvent removal, the product was purified through recrystallization with ethanol, as depicted in Scheme 3.

2.5. *Selected NMR data*

1,1′-biphenyl:^{1}H NMR (400 MHz, DMSO)**:** δ_H= 7.20–7.76 (m, 10H) ppm. M/Z:154.068

[1,1′-biphenyl] −4-amine:^{1}H NMR (400 MHz, DMSO): δ_H= 7.07–7.62 (m, 9H), 5.17 (s, 2H) ppm. M/Z:169.201

4-Methoxy-1,1′-biphenyl:^{1}H NMR (400 MHz, DMSO): δ_H= 7.20–7.73 (m, 9H), 4.01 (s, 3H) ppm. M/Z:184.080

bis(4-methoxyphenyl)sulfane:^{1}H NMR (400 MHz, DMSO): δ_H= 6.86–7.38 (m, 8H), 3.83 (s, 6H) ppm. M/Z:246.071

diphenylsulfane:^{1}H NMR (400 MHz, DMSO): δ_H= 7.51–7.70 (m, 10H) ppm. M/Z:186.050

4,4′-thiodiphenol:^{1}H NMR (400 MHz, DMSO): δ_H= 6.62–6.85 (m,

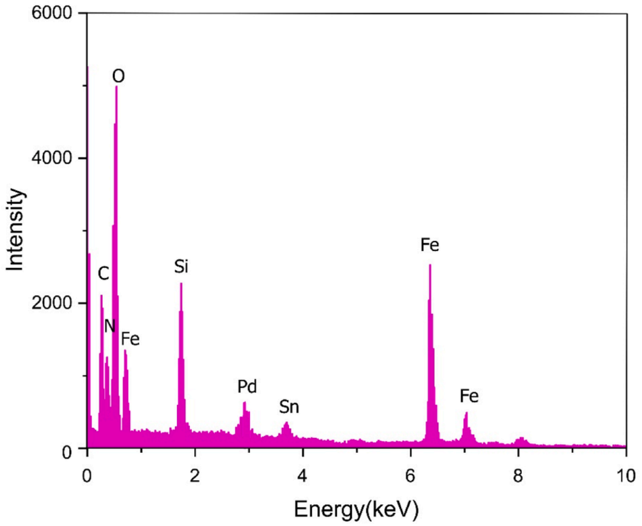

Fig. 4. EDS analysis of $SnFe_2O_4@SiO_2@P\text{-}Pd$.

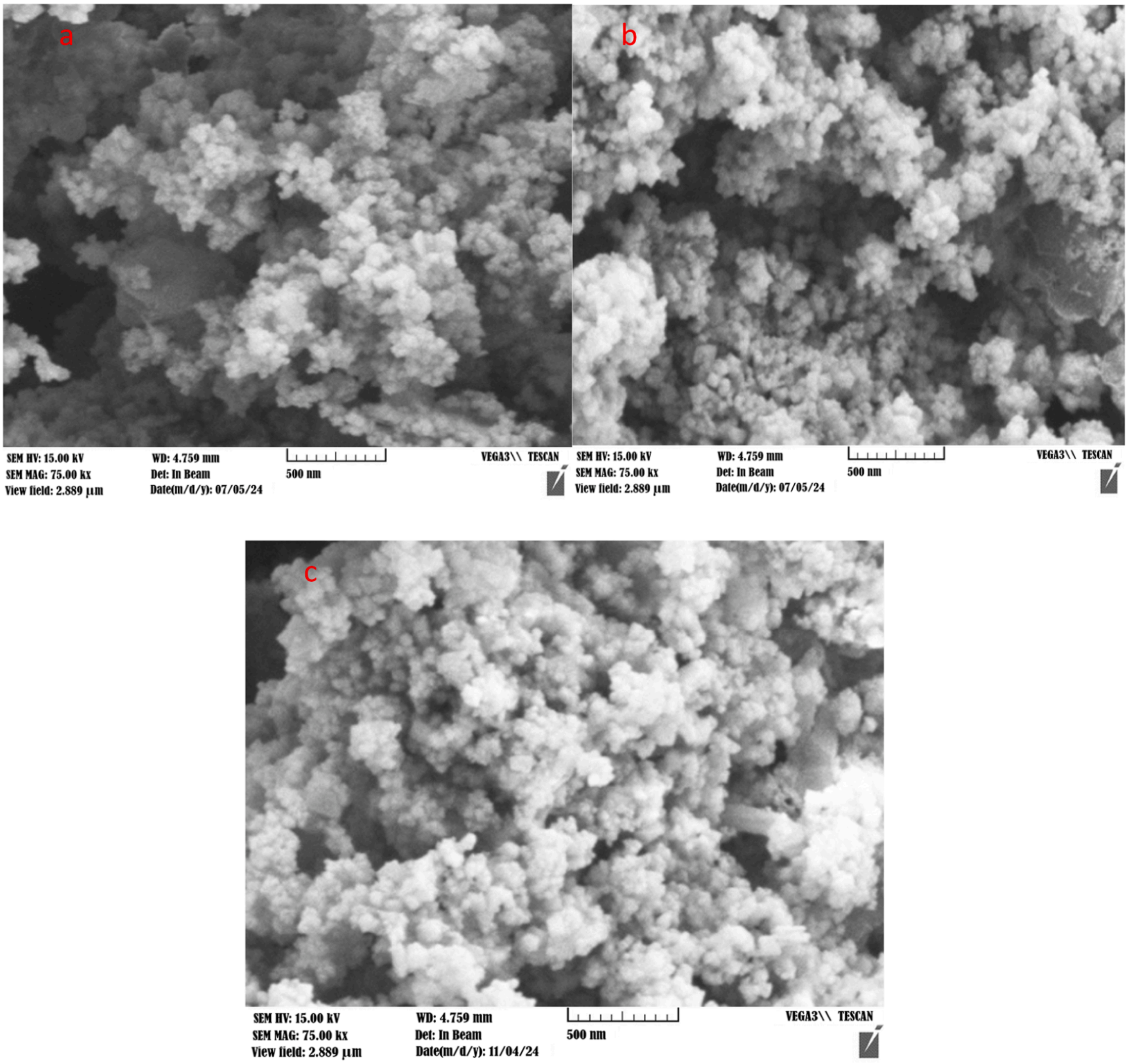

Fig. 5. SEM images of $SnFe_2O_4@SiO_2@P$-Pd (a and b), and recovered catalyst (c).

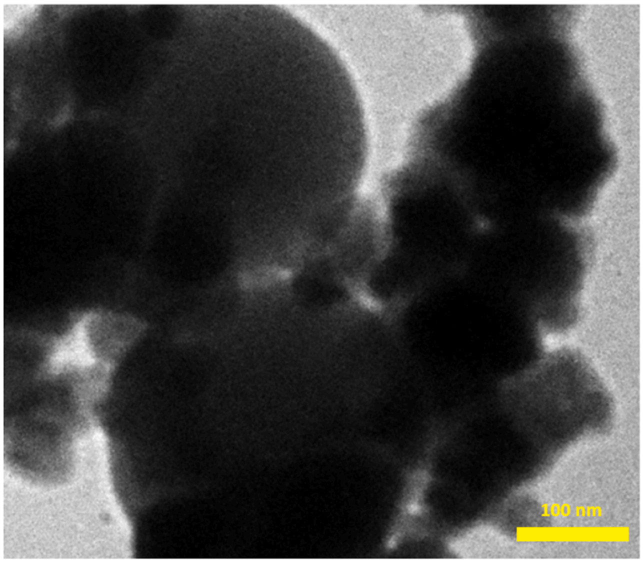

Fig. 6. TEM images of $SnFe_2O_4@SiO_2@P$-Pd.

8H), 8.75 (s, 2H) ppm.

2.6. *Catalyst characterizations*

The prepared $SnFe_2O_4@SiO_2@P$-Pd MNPs was characterized by BET, SEM, XRD, EDS, FT-IR, ICP, TGA and VSM techniques.

To ensure the successful synthesis of $SnFe_2O_4@SiO_2@P$-Pd, FT-IR spectroscopy of all synthesis steps was performed with KBr pellets. The absorption bands for $SnFe_2O_4$ (Fig. 1a), and $SnFe_2O_4@SiO_2$ (Fig. 1b) were consistent with our previous reports respectively. In Fig. 1c, two prominent bands at 2807 and 2966 cm^{-1} are observed, which are assigned to the aliphatic Carbon–Hydrogen stretching of organic ligands. The presence of absorption bands at 1420 cm^{-1} can correspond to Carbon–Nitrogen stretching vibrations, 1547 cm^{-1} and 1673 cm^{-1} are associated with the Carbon- Carbon double bond aromatic ring, which confirm the successful attach. More importantly, the change in the intensity of the peaks of $SnFe_2O_4@SiO_2@P$-Pd (Fig. 1d) confirms the coordination of the nitrogen atom of the amino groups to Pd.

An analysis of the X-ray diffraction (XRD) pattern of $SnFe_2O_4@SiO_2@P$-Pd was conducted, and the comparative data are illustrated in Fig. 2. The results align with the established standards for the $SnFe_2O_4$ crystal structure. Notably, the catalyst's phase morphology remained unchanged throughout the process of grafting the P-Pd complex onto $SnFe_2O_4$.

Thermogravimetric analysis (TGA) is a compelling and effective method for examining the thermal stability of magnetic nanoparticles. This technique is instrumental in confirming and interpreting the bond formation between magnetite nanoparticles and organic complexes. As illustrated in Fig. 3, the initial 9 % weight loss below 250 °C is linked to the removal of physically adsorbed solvents. Meanwhile, the additional 15 % weight loss occurring between 250 °C and 1000 °C corresponds to the decomposition of organic layers on the $SnFe_2O_4$ surface, affirming the successful grafting of organic groups onto the $SnFe_2O_4$ magnetic nanoparticles.

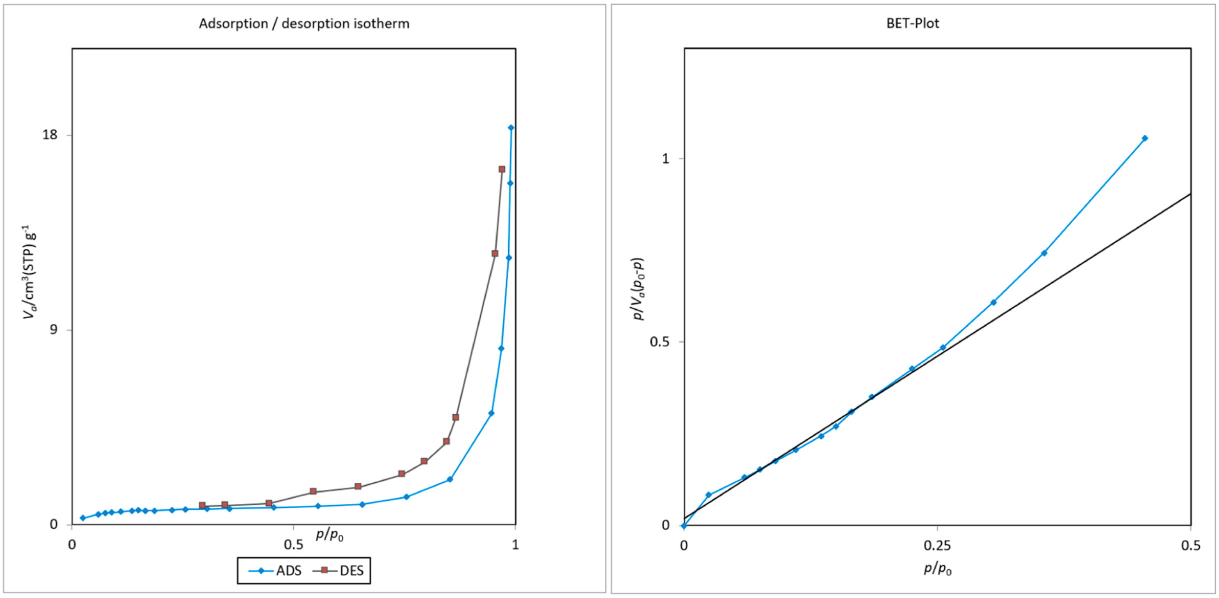

Fig. 7. Adsorption and desorption behavior of the as-synthesized catalyst.

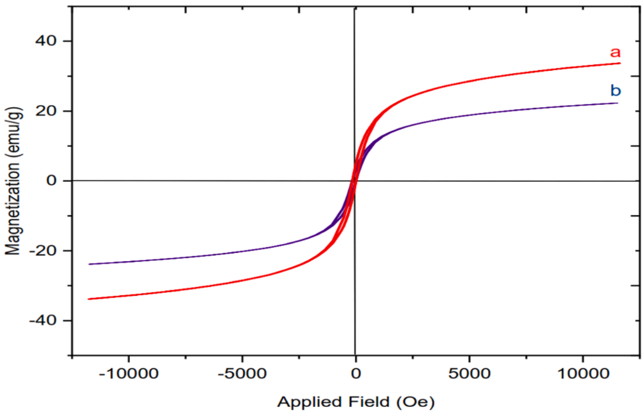

Fig. 8. VSM curves of (a) $SnFe_2O_4$ (b) $SnFe_2O_4@SiO_2@P\text{-}Pd$.

The elemental composition of $SnFe_2O_4@SiO_2@P\text{-}Pd$ was analyzed using EDX. Fig. 4 verifies the presence of Pd, C, Si, N, O, Sn, and Fe in the nanocatalyst, as indicated by the EDX pattern database.

Subsequently, the morphology of $SnFe_2O_4@SiO_2@P\text{-}Pd$ was examined using Scanning Electron Microscopy (SEM), as illustrated in Fig. 5a and b. The images distinctly reveal that the synthesized nanoparticles are structured as fine grains. Fig. 2c presents a comparison of SEM spectra for the catalyst following recycling. As illustrated, the SEM of $SnFe_2O_4@SiO_2@P\text{-}Pd$ remains unchanged after recovery, confirming the stability of this catalyst under the reaction conditions.

To verify the aggregation of nanoparticles, a Transmission Electron Microscopy (TEM) analysis of the synthesized catalyst was conducted. These observations were corroborated with data acquired from the transmission electron microscopy images, as presented in Fig. 6.

To further explore the measurement of the specific surface area of the as-synthesized catalyst, adsorption and desorption isotherms were conducted under a nitrogen atmosphere. Fig. 7 presents these isotherms. By applying the data to the Brunauer–Emmett–Teller (BET) theory, a specific surface area of 3.21 m^2/g and a mean pore diameter of 45.61 nm were obtained. These results suggest potential applications for the as-synthesized catalyst.

Subsequently, utilizing the Inductively Coupled Plasma (ICP) technique, the quantity of palladium within the initial nanocatalyst, as well as the extent of palladium leaching following recycling, was assessed. The results indicate that the palladium content in both fresh and recycled nanocatalysts is 1.4×10^{-4} and 1.2×10^{-4} mol g^{-1}, respectively. This demonstrates that palladium leaching from the $SnFe_2O_4@SiO_2@P\text{-}Pd$ framework is minimal.

The magnetic properties of the (a) $SnFe_2O_4$ and (b) $SnFe_2O_4@SiO_2@P\text{-}Pd$ nanostructures were examined through Vibrating Sample Magnetometer (VSM) analysis conducted at ambient temperature, as illustrated in Fig. 8. The magnetization curves revealed that the saturation magnetization (Ms) values for the (a) $SnFe_2O_4$ and (b) $SnFe_2O_4@SiO_2@P\text{-}Pd$ nanostructures were 33 emu g^{-1} and 22 emu g^{-1}, respectively.

Table 1
Optimization of reaction conditions for carbon-sulfur coupling using 2-thiobarbituric acid and iodobenzene in the presence of $SnFe_2O_4@SiO_2@P\text{-}Pd$ nanocatalyst.

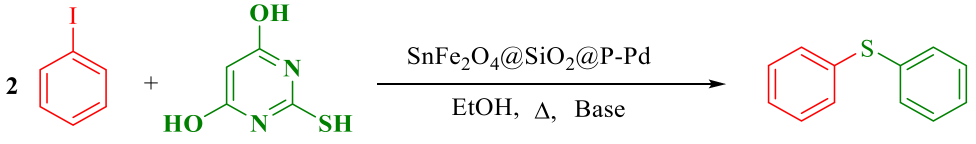

Entry	Catalyst (g)	Solvent	Base	Temperature (°C)	Time (h)	Yield (%)[a, b]
1.	–	EtOH	KOH	Reflux	12 days	N. R
2.	0.01	EtOH	KOH	Reflux	3	42
3.	0.015	EtOH	KOH	Reflux	3	56
4.	0.02	EtOH	KOH	Reflux	3	83
5.	0.03	EtOH	KOH	Reflux	3	96
6.	0.04	EtOH	KOH	Reflux	3	96
7.	0.03	H_2O	KOH	Reflux	3	35
8.	0.03	PEG-200	KOH	Reflux	3	48
9.	0.03	Acetonitrile	KOH	Reflux	3	N. R
10.	0.03	DMSO	KOH	Reflux	3	82
11.	0.03	MeOH	KOH	Reflux	3	90
12.	0.03	EtOH	*t*-BuOK	Reflux	3	40
13.	0.03	EtOH	Na_2CO_3	Reflux	3	65
14.	0.03	EtOH	Et_3N	Reflux	3	88
15.	0.03	EtOH	Cs_2CO_3	Reflux	3	N.R
16.	0.03	EtOH	NaOH	Reflux	3	40
17.	0.03	EtOH	K_2CO_3	Reflux	3	30
18.	0.03[c]	EtOH	KOH	Reflux	3	–

[a] Reaction conditions: 2-thiobarbituric acid (0.5 mmol), iodobenzene (0.5 mmol), $SnFe_2O_4@SiO_2@P\text{-}Pd$ (0.015 g), base (1 mmol).

[b] Isolated yield.

[c] Catalyzed by $SnFe_2O_4@SiO_2@P$.

Table 2
Catalytic coupling reaction of various aryl halides with triphenyltin chloride in the presence of catalytic amounts of $SnFe_2O_4@SiO_2@P\text{-}Pd$.

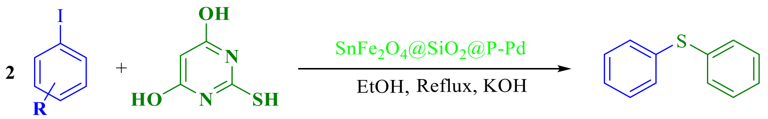

Entry	**Aryl halide**	**Product**	**Time (h)**	**Yield (%)**	**TON**	**TOF (min^{-1})**
1	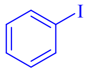	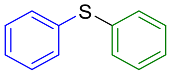	3	96	228	76
2	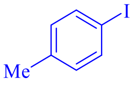	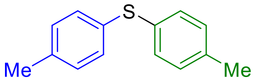	4	84	200	50
3	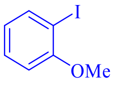	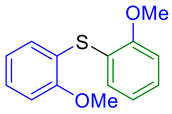	4	70	166	41
4	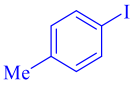	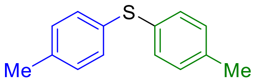	4	75	178	44
5	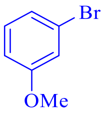	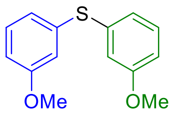	3	90	214	71
6	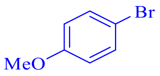	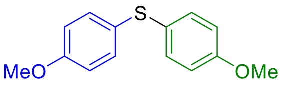	3	94	223	74
7	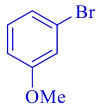	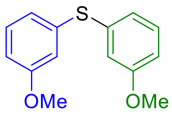	4	85	202	67
8	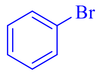	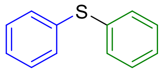	4	80	190	47
9	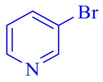	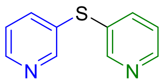	3	94	223	74
10	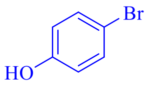	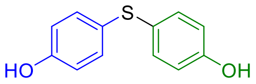	5	35	83	16

(*continued on next page*)

Table 2 (*continued*)

11	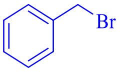	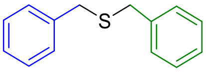	2	95	226	113
12	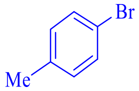	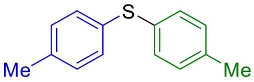	4	75	178	44
13	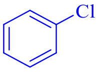	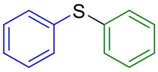	4	35	83	21
14	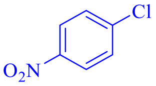	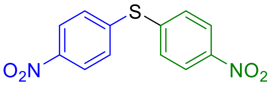	5	50	119	24
15	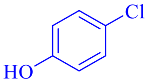	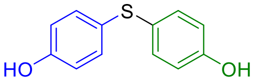	5	40	95	19

2.7. Catalytic studies

Upon successful preparation and characterization of $SnFe_2O_4$@SiO_2@P-Pd, its catalytic efficacy was evaluated in facilitating the synthesis of both biaryl compounds and symmetrical sulfides.

In order to determine the optimal conditions, the catalytic activity of $SnFe_2O_4$@SiO_2@P-Pd was investigated through its application in the reaction between 2-thiobarbituric acid and iodoarene, serving as a model reaction. As illustrated in Table 1, an initial examination of the reaction parameters was conducted. This included assessing the influence of temperature, various solvents, and the quantities of base and catalyst utilized. The most favorable outcomes were observed when using KOH as the base, with 0.03 g of $SnFe_2O_4$@SiO_2@P-Pd magnetic nanoparticles in 4 ml of ethanol under reflux conditions.

As illustrated in Table 2, we explored the range of substrates under the optimized reaction conditions. To demonstrate the chemoselectivity of the proposed protocol, a diverse array of aryl halide derivatives was synthesized under optimal conditions. The reactions involving both electron-rich and electron-deficient aryl halides successfully produced the corresponding sulfide derivatives with excellent yields, regardless of the electronic properties of the substituents.

Previous reports detail the catalytic cycle for synthesizing symmetrical sulfides using $SnFe_2O_4$@SiO_2@P-Pd, as illustrated in Scheme 3. Initially, 2-thiobarbituric acid reacts with potassium hydroxide to yield potassium thiolate. Subsequently, an aryl halide undergoes oxidative addition with palladium, forming intermediate (I). Following this, potassium thiolate interacts with intermediate (I) to create intermediate (II). This is then converted into a thiol anion in the presence of potassium

Table 3
Optimization of the reaction conditions for the coupling reaction of iodobenzene with triphenyltin chloride in the presence of $SnFe_2O_4$@SiO_2@P-Pd.

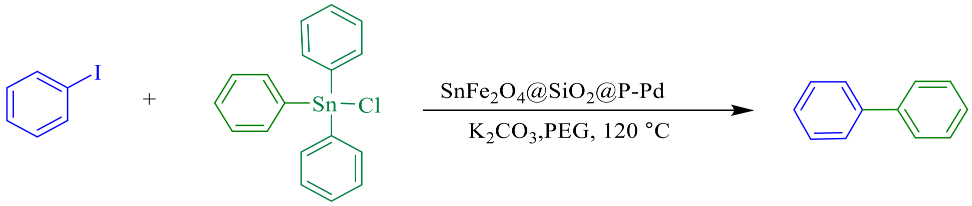

Entry	Catalyst (g)	Solvent	Base	Temperature (°C)	Time (min)	Yield (%)
1	–	PEG	K_2CO_3	120	1 day	N. R
2	0.005	PEG	K_2CO_3	120	25	50
3	0.01	PEG	K_2CO_3	120	25	81
4	0.02	PEG	K_2CO_3	120	25	93
5	0.03	PEG	K_2CO_3	120	25	97
6	0.035	PEG	K_2CO_3	120	25	97
7	0.03	H_2O	K_2CO_3	120	25	36
8	0.03	hexane	K_2CO_3	120	25	48
9	0.03	Acetonitrile	K_2CO_3	120	25	75
10	0.03	EtOAc	K_2CO_3	120	25	82
11	0.03	EtOH	K_2CO_3	120	25	92
12	0.03	PEG	Cs_2CO_3	120	25	85
13	0.03	PEG	Et_3N	120	25	82
14	0.03	PEG	NaOH	120	25	42
15	0.03	PEG	KOH	120	25	32
16	0.03[a]	PEG	K_2CO_3	120	25	–

[a] Catalyzed by $SnFe_2O_4$@SiO_2@P.

Table 4
Catalytic coupling reaction of various aryl halides with triphenyltin chloride in the presence of catalytic amounts of $SnFe_2O_4@SiO_2@P\text{-}Pd$.

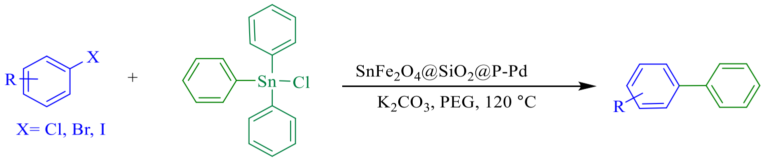

Entry	Aryl halide	Product	Time (min)	Yield (%)	TON	TOF (min^{-1})
1	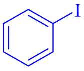	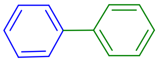	25	97	233	557
2	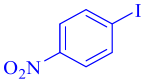	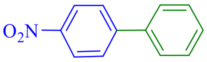	40	91	216	360
3	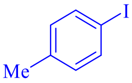	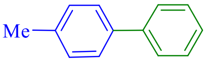	45	92	219	292
4	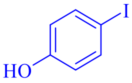	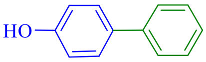	20	91	216	720
5	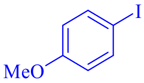	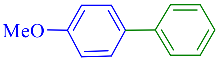	20	90	214	713
6	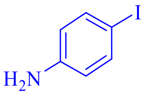	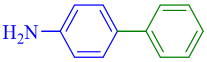	30	96	228	456
7	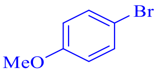	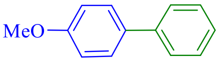	60	95	226	226
8	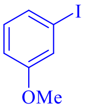	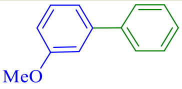	30	96	228	456
9	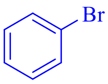	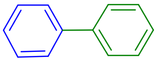	55	91	216	237
10	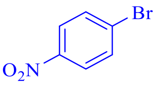	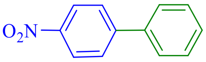	25	90	214	521

(continued on next page)

Table 4 (*continued*)

11	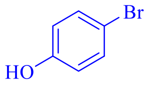	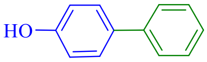	30	94	223	446
12	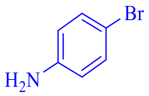	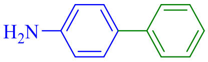	65	94	223	171
13	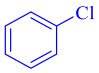	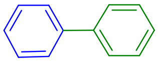	30	91	216	432
14	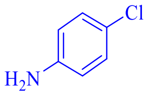	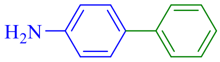	130	85	202	96
15	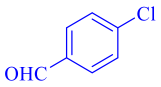	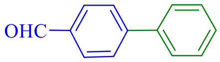	55	67	159	73
16	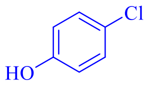	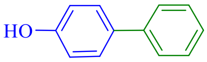	95	91	216	135

hydroxide. The thiol anion further reacts with intermediate (I) through oxidative addition, resulting in compound (III), which is then reduced. Upon completion, the catalytic cycle resumes with the release of $SnFe_2O_4@SiO_2@P$-Pd.

The subsequent step involved using the reaction between iodobenzene and triphenyltin chloride as the model reaction. By fine-tuning the catalyst quantity and selecting the suitable base and solvent, along with careful temperature control and timing, the reaction progression and product yield were improved. As illustrated in Table 3, by repeating the experiment under varying conditions, K_2CO_3 (2.5 mmol) emerged as the ideal base, with PEG serving as the solvent for the reaction. It's important to note that altering the catalyst amount significantly impacts the reaction. Conducting the reaction with different bases led to reduced efficiency. Based on the results, the optimal conditions for this reaction involve a catalyst amount of 0.03 g and K_2CO_3 (2.5 mmol) as the base in PEG at 120 °C.

After determining the ideal conditions for the coupling reaction between triphenyltin chloride and iodobenzene (C_6H_5I), research was expanded to explore the catalytic potential of $SnFe_2O_4@SiO_2@P$-Pd in reactions involving other aryl halides and triphenyltin chloride. The study included various aryl chlorides, bromides, and iodides in coupling reactions with triphenyltin chloride, facilitated by $SnFe_2O_4@SiO_2@P$-Pd. Aryl halides with both electron-rich and electron-poor characteristics were used in acetylation reactions, successfully yielding the desired biphenyl derivatives with yields ranging from 67 % to 98 %, as detailed in Table 4.

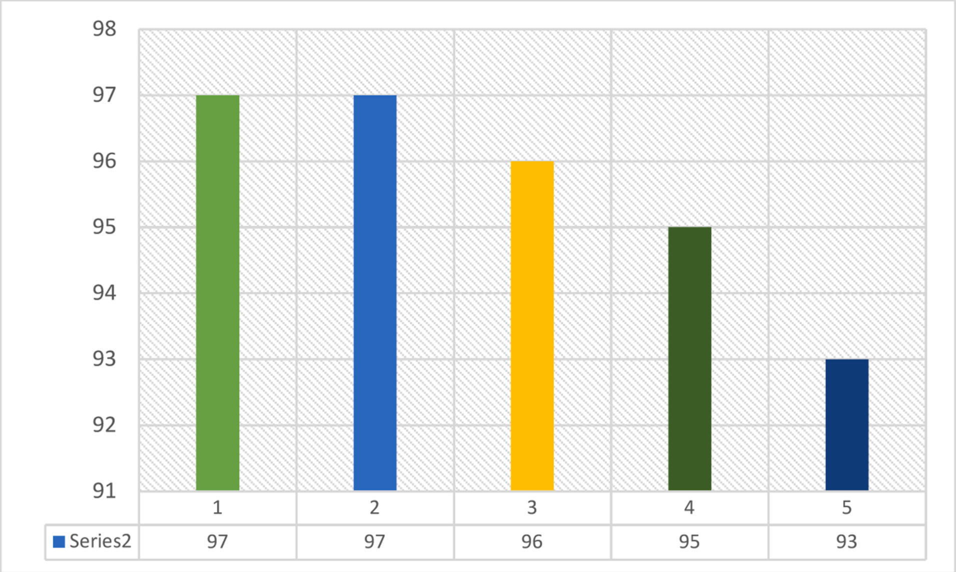

Fig. 9. Recyclability of $SnFe_2O_4@SiO_2@P$-Pd in the synthesis of Stille reaction.

Table 5
Comparing catalytic activity of $SnFe_2O_4@SiO_2@P\text{-}Pd$ with previously reported methods in the Stille reaction.

Entry	Ar-X	Cat.	**Condition reaction**	T (min)	Yield (%)	Ref.
1	Iodobenzene	Pd-BTU	NaOAc, PEG-400, 25 °C	1 h	94	[22]
2	Iodobenzene	MNPs Pd-Fe_3O_4	DMF, K_2CO_3, 100 °C	10 h	95	[23]
3	Iodobenzene	$Fe_3O_4@SiO_2@NHCSPh\text{-}Pd(II)$	DMF, K_2CO_3, 90 °C	6 h	95	[24]
4	Iodobenzene	Pd NPs	PEG, K_2CO_3, H_2O, 80 °C	1 h	90	[25]
5	Iodobenzene	$SnFe_2O_4@SiO_2@P\text{-}Pd$	EtOH, K_2CO_3, 60 °C	25	97	This work

Drawing upon previous studies and the aforementioned evidence, the catalytic cycle for the Stille reaction in the presence of $SnFe_2O_4@SiO_2@P\text{-}Pd$ is depicted in Scheme 5. Amines, functioning as electron-donating groups on the Phenylalanine ligand, play a crucial role in activating Pd(0). The process initiates with the oxidative addition of aryl halides to the $SnFe_2O_4@SiO_2@P\text{-}Pd$ complex, resulting in the formation of intermediate 1. Subsequently, the Ar-X bond within the catalyst is cleaved, facilitating the establishment of Pd-Ar and Pd-X bonds. In the third stage, an organoborane compound undergoes transmetalation with intermediate 1, in the presence of a base, producing intermediate 2. This series of reactions culminates in the final step, yielding product 3.

3. Catalyst recyclability

Subsequently, to evaluate the stability of the catalyst's activity, the reaction between aryl iodide (C_6H_5I) and triphenyltin chloride was utilized as a model system in ethanol, employing 0.03 g of $SnFe_2O_4@SiO_2@P\text{-}Pd$. The synthesized nanocatalyst was conveniently recovered using a magnet, as detailed in the experimental methodology. Remarkably, the catalyst $SnFe_2O_4@SiO_2@P\text{-}Pd$ was reused over five consecutive cycles without any diminishment in catalytic performance, as illustrated in Fig. 9.

In the following step, the behavior of different nanocatalysts is compared with $SnFe_2O_4@SiO_2@P\text{-}Pd$ in the Stille reaction, as documented in the literature and summarized in Table 5. According to Table 5, the $SnFe_2O_4@SiO_2@P\text{-}Pd$ nanocatalyst demonstrates greater efficiency than the other catalysts mentioned.

4. Conclusion

In this study, we have successfully developed $SnFe_2O_4@SiO_2@P\text{-}Pd$ as a novel and environmentally friendly recoverable catalyst. Comprehensive characterization of the synthesized catalyst was conducted using BET surface area analysis, Fourier-transform infrared spectroscopy (FTIR), X-ray diffraction (XRD), transmission electron microscopy (TEM), energy-dispersive X-ray spectroscopy (EDS), thermogravimetric analysis (TGA), vibrating sample magnetometry (VSM), scanning electron microscopy (SEM), and inductively coupled plasma (ICP) techniques. The catalyst demonstrated significant activity across a diverse array of substrates, exhibiting a high turnover frequency. Its facile recyclability contributes to its cost-effectiveness and appeal in addressing environmental concerns. The catalyst was effectively

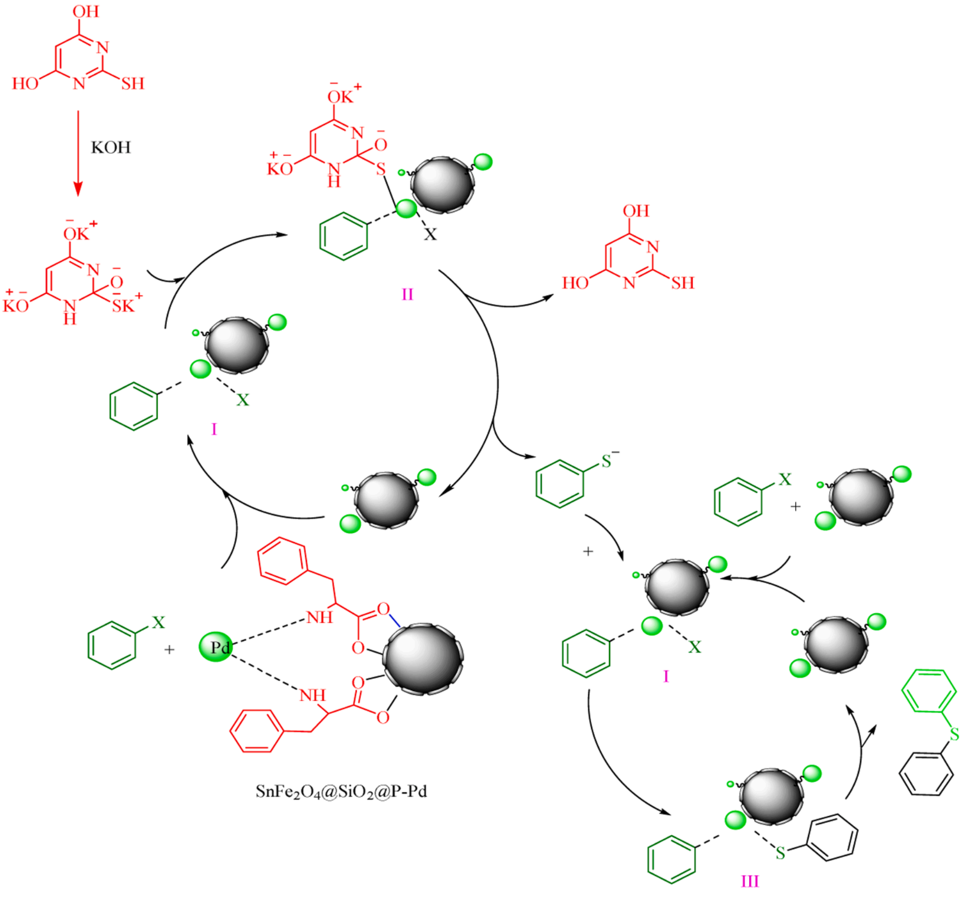

Scheme 4. Proposed mechanisms for the synthesis of symmetrical sulfides.

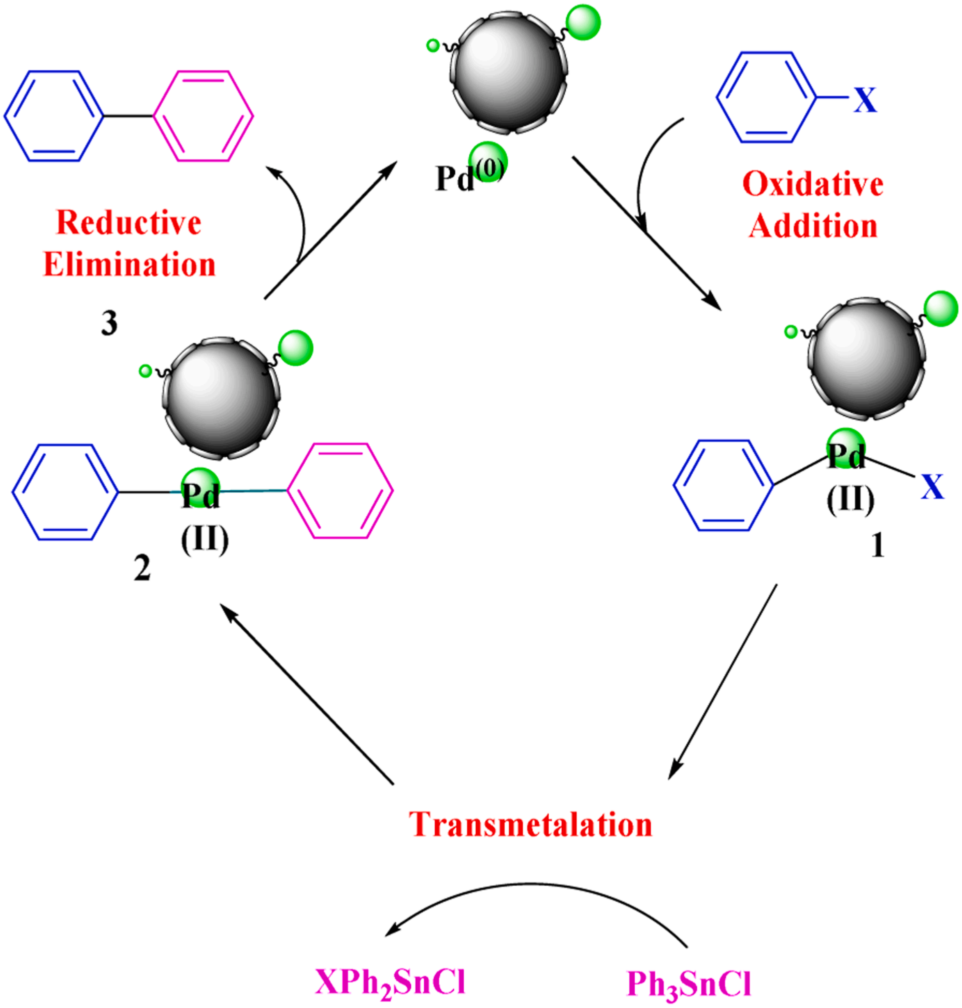

Scheme 5. Proposed mechanism for Stille reaction.

employed in the synthesis of symmetrical sulfides and utilized in the Stille reaction. Furthermore, the nanocatalyst offers advantages in terms of reusability, easy separation, and robust catalytic performance (Scheme 4).

CRediT authorship contribution statement

Anjan Kumar: Writing – review & editing, Software, Investigation. **Jayanti Makasana:** Writing – original draft, Software, Resources. **Suhas Ballal:** Project administration, Methodology, Investigation. **Hamidah Abu Bakar:** Resources, Project administration, Methodology, Investigation. **Girish Chandra Sharma:** Writing – original draft, Supervision, Methodology. **RSK Sharma:** Writing – review & editing, Validation, Supervision, Resources. **Lakshay Bareja:** Visualization, Methodology, Investigation. **Salwa Bader AlReshaidan:** Software, Project administration, Methodology. **Mohammed A. El-Meligy:** Writing – original draft, Visualization, Validation. **Munthar Kadhim Abosaoda:** Project administration, Funding acquisition, Data curation.

Declaration of competing interest

The authors collectively affirm that they possess no financial conflicts of interest or personal affiliations that could potentially affect the integrity of this research project.

Acknowledgements

The authors present their appreciation to King Saud University for funding this research through Researchers Supporting Project number (RSPD2024R779), King Saud University, Riyadh, Saudi Arabia.

Supplementary materials

Supplementary material associated with this article can be found, in the online version, at doi:10.1016/j.molstruc.2024.140803.

Data availability

All data produced in this article, along with the supplementary information files, have been published.

References

[1] H. Batmani, N. Noroozi Pesyan, F. Havasi, Synthesis and characterization of MCM-41-Biurea-Pd as a heterogeneous nanocatalyst and using its catalytic efficacy in C–C, C–N and C–O coupling reactions, Appl. Organomet. Chem. 32 (2018) e4419, https://doi.org/10.1002/aoc.4419.

[2] A. Mohammadkhanni, A. Bazgir, Palladium supported SBA-functionalizd 1,2-dicarboxylic acid: the first Pd-based heterogeneous synthesis of fluorenones, Mol. Catal. 447 (2018) 28–36, https://doi.org/10.1016/j.mcat.2017.12.035.

[3] S. Jabeen, R.A. Khera, J. Iqbal, M. Asgher, Design, synthesis and application of triazole ligands in suzuki miyaura cross coupling reaction of aryl chlorides, J. Mol. Struct. 1206 (2020) 127753, https://doi.org/10.1016/j.molstruc.2020.127753.

[4] S.P. Vibhute, P.M. Mhaldar, R.V. Shejwal, D.M. Pore, Magnetic nanoparticles-supported palladium catalyzed Suzuki-Miyaura cross coupling, Tetrahedron Lett. 61 (2020) 151594, https://doi.org/10.1016/j.tetlet.2020.151594.

[5] Z. Nawaz, N. Gürbüz, M.N. Zafar, N. Özdemir, U. Habib, K. Jan, I. Özdemir, Synthesis of new Pd(NHC)-PEPPSI type complexes as catalysts toward C-C cross-coupling reactions, J. Mol. Struct. 1243 (2021) 130883, https://doi.org/10.1016/j.molstruc.2021.130883.

[6] S. Gorji, R. Ghorbani-Vaghei, Ag nanoparticles stabilized on basalt fibers as a novel, stable, and reusable catalyst for Suzuki–Miyaura coupling reactions, Appl. Organomet. Chem. 35 (2021), https://doi.org/10.1002/aoc.6018.

[7] C. Han, R. Qi, R. Sun, K. Fan, B. Johannessen, D.-C. Qi, S. Cao, J. Xu, Enhanced support effects in single-atom copper-incorporated carbon nitride for photocatalytic suzuki cross-coupling reactions, Appl. Catal. B: Environ. 320 (2023) 121954, https://doi.org/10.1016/j.apcatb.2022.121954.

[8] Z. Shirvandi, A. Rostami, Immobilized zirconium-thiouracil complex on MCM-41 magnetic mesoporous as a recyclable nanocatalyst for carbon-sulfide bond formation, Appl. Organomet. Chem. 38 (2024) e7321, https://doi.org/10.1002/aoc.7321.

[9] S. Sunitha, B. Rajakumar, A computational study on the kinetics of OH radical reactions with fluorinated dimethyl sulfides in the atmospheric window, Chem. Phys. Lett. 851 (2024) 141478, https://doi.org/10.1016/j.cplett.2024.141478.

[10] C.L. Ong, W.K. Tang, N.G. Khaligh, J.C. Juan, One-pot thermo-induced radical-radical oxidative cross-coupling for symmetrical dimeric thiadiazole monosulfide formation, J. Mol. Struct. 1301 (2024) 137389, https://doi.org/10.1016/j.molstruc.2023.137389.

[11] A. Ghaderi, F. Abdollahi, M. Biglari, Copper-sulfur interactions leading to the formation of S-containing compounds, Tetrahedron Lett. 143 (2024) 155112, https://doi.org/10.1016/j.tetlet.2024.155112.

[12] N. Sun, K. Zheng, M. Zhang, G. Zheng, L. Jin, B. Hu, Z. Shen, X. Hu, Cu-catalysed Chan–Lam synthesis of unsymmetrical aryl chalcogenides under aqueous micellar conditions, Green Chemistry 25 (2023) 2782–2789, https://doi.org/10.1039/D3GC00051F.

[13] R. Lei, W. Lan, M. Li, B. Fu, A convenient approach to benzosultam-linked pyrazole compounds, Chin. J. Org. Chem. 43 (2023) 2553–2560, https://doi.org/10.6023/cjoc202209009.

[14] L. Wang, Y.-B. Xie, Q.-L. Yang, M.-G. Liu, K.-B. Zheng, Y. Hu, N.-Y. Huang, Ir-catalyzed C–S coupling of quinones with sulfonyl chloride, J. Iran. Chem. Soc. 13 (2016) 1797–1803, https://doi.org/10.1007/s13738-016-0897-8.

[15] N. Muhammad, S. Nadeem, Ferrite nanoparticles Ni- ZnFe2O4, Mn- ZnFe2O4 and Fe2O4 in the flow of ferromagnetic nanofluid, Eur. Phys. J. Plus. 132 (2017), https://doi.org/10.1140/epjp/i2017-11650-2.

[16] N. Hadrup, A.T. Saber, Z.O. Kyjovska, N.R. Jacobsen, M. Vippola, E. Sarlin, Y. Ding, O. Schmid, H. Wallin, K.A. Jensen, U. Vogel, Pulmonary toxicity of Fe2O3, ZnFe2O4, NiFe2O4 and NiZnFe4O8 nanomaterials: inflammation and DNA strand breaks, Environ. Toxicol. Pharmacol. 74 (2020) 103303, https://doi.org/10.1016/j.etap.2019.103303.

[17] C. Singh, R.Malik Devika, V. Kumar, S. Singhal, CdS nanorod-MFe2O4 (M = Zn, Co and Ni) nanocomposites: a heterojunction synthesis strategy to mitigate environmental deterioration, RSC Adv. 5 (2015) 89327–89337, https://doi.org/10.1039/c5ra13837j.

[18] R.A. Henning, P. Uredat, C. Simon, A. Bloesser, P. Cop, M.T. Elm, R. Marschall, Characterization of MFe2O4 (M = Mg, Zn) thin films prepared by pulsed laser deposition for photoelectrochemical applications, J. Phys. Chem. C 123 (2019) 18240–18247, https://doi.org/10.1021/acs.jpcc.9b04635.

[19] T. Li, T. Yang, Z. Yu, G. Xu, M. Du, Y. Guan, C. Guo, An innovative magnetic bar separator for removal of chromium ions in tanning wastewater, J. Water. Process. Eng. 40 (2021), https://doi.org/10.1016/j.jwpe.2021.101916.

[20] N. Muniyappan, S. Sabiah, Synthesis, structure, and characterization of picolyl- and benzyl-linked biphenyl palladium N-heterocyclic carbene complexes and their catalytic activity in acylative cross-coupling reactions, Appl. Organomet. Chem. 34 (2020), https://doi.org/10.1002/aoc.5421.

[21] H. Alamgholiloo, S. Rostamnia, N. Noroozi Pesyan, Extended architectures constructed of thiourea-modified SBA-15 nanoreactor: a versatile new support for the fabrication of palladium pre-catalyst, Appl. Organomet. Chem. 34 (2020), https://doi.org/10.1002/aoc.5452.

[22] H. Alamgholiloo, S. Rostamnia, N.N. Pesyan, Anchoring and stabilization of colloidal PdNPs on exfoliated bis-thiourea modified graphene oxide layers with super catalytic activity in water and PEG, Colloids Surf. A: Physicochem. Eng. Asp. 602 (2020) 125130, https://doi.org/10.1016/j.colsurfa.2020.125130.

[23] B.S. Kumar, R. Anbarasan, A.J. Amali, K. Pitchumani, Isolable C@Fe3O4 nanospheres supported cubical Pd nanoparticles as reusable catalysts for Stille and Mizoroki-Heck coupling reactions, Tetrahedron. Lett. 58 (2017) 3276–3282, https://doi.org/10.1016/j.tetlet.2017.07.025.

[24] H. Khandaka, K.N. Sharma, R.K. Joshi, Aerobic Cu and amine free sonogashira and stille couplings of aryl bromides/chlorides with a magnetically recoverable Fe3O4@SiO2 immobilized Pd(II)-thioether containing NHC, Tetrahedron. Lett. 67 (2021) 152844, https://doi.org/10.1016/j.tetlet.2021.152844.

[25] W.-J. Zhou, K.-H. Wang, J.-X. Wang, Pd(PPh3)4-PEG 400 Catalyzed protocol for the atom-efficient stille cross-coupling reaction of organotin with aryl bromides, J. Org. Chem. 74 (2009) 5599–5602, https://doi.org/10.1021/jo9005206.